

Tant, Katherine M. M.; Mulholland, Anthony J.; Curtis, Andrew; Ijomah, Winifred L.

Article

Design-for-testing for improved remanufacturability

Journal of Remanufacturing

Provided in Cooperation with:

Springer Nature

Suggested Citation: Tant, Katherine M. M.; Mulholland, Anthony J.; Curtis, Andrew; Ijomah, Winifred L. (2019) : Design-for-testing for improved remanufacturability, Journal of Remanufacturing, ISSN 2210-4690, Springer, Heidelberg, Vol. 9, Iss. 1, pp. 61-72,
<https://doi.org/10.1007/s13243-018-0057-7>

This Version is available at:

<https://hdl.handle.net/10419/232981>

Standard-Nutzungsbedingungen:

Die Dokumente auf EconStor dürfen zu eigenen wissenschaftlichen Zwecken und zum Privatgebrauch gespeichert und kopiert werden.

Sie dürfen die Dokumente nicht für öffentliche oder kommerzielle Zwecke vervielfältigen, öffentlich ausstellen, öffentlich zugänglich machen, vertreiben oder anderweitig nutzen.

Sofern die Verfasser die Dokumente unter Open-Content-Lizenzen (insbesondere CC-Lizenzen) zur Verfügung gestellt haben sollten, gelten abweichend von diesen Nutzungsbedingungen die in der dort genannten Lizenz gewährten Nutzungsrechte.

Terms of use:

Documents in EconStor may be saved and copied for your personal and scholarly purposes.

You are not to copy documents for public or commercial purposes, to exhibit the documents publicly, to make them publicly available on the internet, or to distribute or otherwise use the documents in public.

If the documents have been made available under an Open Content Licence (especially Creative Commons Licences), you may exercise further usage rights as specified in the indicated licence.



<https://creativecommons.org/licenses/by/4.0/>



Design-for-testing for improved remanufacturability

Katherine M. M. Tant¹  · Anthony J. Mulholland¹ · Andrew Curtis² · Winifred L. Ijomah³

Received: 13 December 2017 / Accepted: 30 August 2018 / Published online: 10 September 2018
© The Author(s) 2018

Abstract

By definition, a remanufactured product must perform to the same (or higher) level as the original product, and must therefore be issued a warranty of the same (or longer) duration. However, many components of remanufactured products will have been subjected to regular stresses in their first cycle of use and may exhibit unseen signs of damage at a microstructural level. This may not affect the remanufactured product's performance initially but could cause it to fail before its renewed warranty expires. To combat this, we propose that the integrity of individual components is assessed non-destructively before they are consigned to storage. However, lack of remanufacture specific tools and techniques for assessment, particularly non-destructive tools, are major hindrances to this strategy. Furthermore, ease of non-destructive testing (NDT) is not currently a consideration in the design of components; components with complex geometries may therefore be difficult to test. This preview paper presents, for the first time, a framework for including NDT suitability as a design criterion at the outset of the component's lifecycle, where the geometry and surface accessibility of the component are optimised for future assessment. Ensuring that components can be easily inspected would not only allow increased confidence in the structural integrity of remanufactured products, but it would also extend the range of products suitable for remanufacturing. This paper serves as a proof of concept, examining simple inspection scenarios in order to demonstrate how the shape of components and data acquisition geometries can adversely affect the coverage of ultrasonic NDT.

Keywords Design for remanufacture · Non-destructive testing · Ultrasonics · Optimisation · Sensors · Product design

Introduction

The majority of remanufacturing processes described in the literature follow a similar procedure: the cores are stripped; components are cleaned, visually assessed, remanufactured and

✉ Katherine M. M. Tant
katy.tant@strath.ac.uk

stored; then the product is rebuilt and its performance tested [13, 16, 21]. Due to a shortage of remanufacture-specific tools and expertise for the non-destructive inspection of these components [11], their integrity is often assessed by their exterior appearance and functional performance. Although it might meet initial performance criteria, interior damage of the structure caused by the strains and stresses experienced in the component's earlier life-cycles could lead to a shorter lifetime than predicted [14]. Full microstructural assessment at the remanufacturing stage would allow increased confidence in the component's integrity and would allow remanufacturing processes to be more readily rolled out to components in high stress environments such as those found in the aerospace and energy industries.

Non-destructive testing (NDT) is an umbrella term for a wide range of analysis techniques used to evaluate and characterise components non-invasively [19]. They are employed to detect defects, take thickness measurements and characterise the internal material properties of components. These techniques include liquid penetrant testing, electromagnetic testing, x-ray computed tomography and infrared and thermal testing [19]. Ultrasonic NDT uses high frequency mechanical waves to inspect components, ensuring that they operate reliably without compromising their integrity [22]. It has grown in popularity within the NDT industry in recent years due to the relatively inexpensive and portable equipment required, and its potential for automation and real-time results [2]. There already exists a large and varied literature on the applications of ultrasonic NDT, and the imaging algorithms required to process the collected ultrasonic data are under constant development [8, 24].

Although ultrasonic cleaning of remanufacturing cores has been investigated in the past [4, 15], ultrasonic non-destructive testing is not currently applied within the remanufacturing process. However, in [20], it was shown that the overall processing times of complex engine parts and the amount of process scrap was significantly reduced when the level of inspection at the *Receive Core* stage of remanufacture was increased. Although this study was limited to application of visual and scent inspection, and fibre optic endoscopy of interior surfaces, it provides evidence that further integration of reliable NDT at the initial stage will enhance the overall process efficiency. This is in line with the Poka-yoke system discussed in [23] which is based on the concept that production costs are reduced by ensuring defects are not propagated through the manufacturing process, but are addressed as they occur.

Although there is an increased pay off in extending the inspection protocols for complex components, complex component geometries and composite material microstructures present significant challenges for the successful application of ultrasonic NDT. To combat this difficulty and improve the ease with which NDT can be applied within the remanufacturing process, we propose a framework for including NDT suitability as a consideration in the component's initial design. By varying the shape and distribution of material within a component, we can maximise the coverage of the ultrasonic field over the structure and minimise the area of dead zones (areas which are not probed by the transmitted wave), thus improving our ability to reliably image internal features of the component.

This design-for-testing proposition aligns with the principles of design for remanufacturing (DfREM), which recognises that a product's design can have a profound impact on its remanufacturing efficiency [12]. Many approaches to implement DfREM have been proposed in the existing literature, including design for disassembly, design for multiple lifecycles, design for upgrade and design for evaluation [12]. The latter approach, design for evaluation, is centred on the designing of products so that their usage can be monitored via record keeping or sacrificial parts, thus allowing the effects of wear and tear

to be estimated. Our proposed design-for-testing framework is similar only in that the primary objective is to assess the internal wear and tear of components. However, we propose that the ability to implement quantitative NDT on a product will provide a more reliable assessment of a component's structural integrity than previously proposed design for evaluation strategies.

Optimal structural design is of particular importance to the aerospace, automotive and civil engineering industries [9]. It is typically used to produce economical, lightweight and robust design solutions whilst adhering to size, weight and topological constraints. Often, an optimisation problem requires the minimisation of more than one variable. For example, companies may often want to look for a structural solution which is both lightweight and low-cost. Thus we have to deal with a multi-objective design optimisation [10]. In this paper, we propose that NDT suitability is introduced as a secondary objective where the subset of solutions shown to be optimal for the existing objectives within a design process are subjected to an optimisation scheme which focusses on maximising the coverage of the ultrasonic field throughout the component whilst minimising the number of ultrasonic transducers required to achieve this (which are also subject to the restrictions on access to its surface). More sophisticated design criteria from the field of experimental design can also be adopted as desired [5, 6]. Design-for-testing has only recently emerged as an important research area [17], whilst design-for-testing for improved remanufacturability has never before been considered. Thus the ideas presented in this paper are cutting edge and the framework developed here will form the basis for future research in the area. As this work is the first of its kind in the area, a novel multi-level optimisation framework, in which both the shape of the component and the location of the ultrasonic transducers are optimised, is proposed. A novel cost function based on the minimum of the pressure field across the component is presented. Inspection scenarios are then simulated for a range of irregularly shaped components as a proof of concept, demonstrating how this cost function depends on the extent of the array aperture and the convexity and surface smoothness of the component. It is hoped that by implementing this approach, not only will the success of in service inspections be enhanced, but the range of products which are suitable for remanufacturing at the end of their first life cycle will be extended.

Methods

Optimisation of the component design

When a component with domain Ω is submitted to ultrasonic NDT, a mechanical force is typically induced at a set of points x on the component's boundary $\partial\Omega$. We consider the coverage of the resulting pressure field throughout the component, which is dependent on the source placement and the component's geometry and material properties. The pressure measured at a point $y \in \Omega$, denoted here as $z(y, t)$, can be written

$$z(y, t) = F(y, t, \theta, \partial\Omega, x) \quad (1)$$

where F is some model of the wave process which is dependent on time t and material properties θ . In this work, a finite element simulation of the wave propagation will be used as our model F [18]. To obtain a map $M(y)$ of the coverage, the maximum pressure amplitude

observed over all t at each point y is plotted. The coverage map is used as a proxy for the ease with which NDT can be applied and is quantified here by

$$\phi = \min_{y \in \Omega} M(y) = \min_{y \in \Omega} \max_{t \in \mathbb{R}^+} |z(y, t)|. \tag{2}$$

Note that alternative measures of the map M may be explored; for example the mean value of the pressure field throughout the component, and the number of points in the domain Ω which lie above some pre-determined threshold relative to the total number of points, are examined in the **Results** section of this paper.

By introducing more sources at different locations on the component’s boundary, we can modify the overall coverage of the component as we are effectively illuminating it from an increased range of angles. To incorporate this, we introduce a probability density function $\xi(x)$ which describes the likelihood that a source is placed at point x on the component boundary (see Fig. 1). Taking, for the moment, the material properties θ to be fixed, we now have all of the ingredients required to define a design criterion function:

$$\Psi(\xi(x), \partial\Omega) = \min_{y \in \Omega} \max_{t \in \mathbb{R}^+} \int_{\partial\Omega} |z(y, t; \theta, \partial\Omega, x)| \xi(x) dx. \tag{3}$$

Here, integrating over x allows us to effectively sum the contributions from all sources, and this is weighted by the probability density function $\xi(x)$ to give an expected value. As before, the maximum value at y over all t is taken (this is effectively map M) of which the minimum is taken as the coverage measure $\Psi(\xi(x), \partial\Omega)$. As we are optimising over two parameters: the shape of the component and the placement of sources, the second of which is dependent on the first, we adopt a bi-level optimisation approach. To clarify this approach, we initially isolate the upper level optimisation.

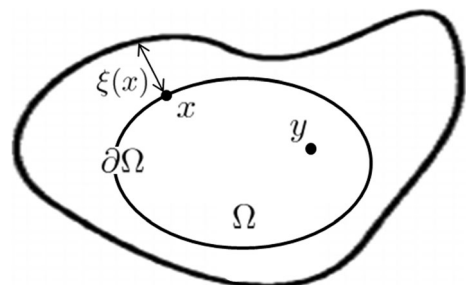
Problem 1: Optimising the component design

We first of all wish to maximise $\Psi(\xi(x), \partial\Omega)$ by finding the optimal admissible boundary design $\partial\Omega^*$ given by

$$\partial\Omega^* = \arg \max_{\partial\Omega \in D} \Psi(\xi(x), \partial\Omega), \tag{4}$$

where D is the set of admissible component boundary geometries (subject to the initial design constraints set by the product manufacturer). For this upper level optimisation, we study the full aperture immersion testing scenario (see Fig. 2a) where the irregularly shaped component is placed in a rectangular water bath and encircled by sources. This allows us to isolate the

Fig. 1 Schematic of an arbitrary component geometry Ω . The perpendicular distance of the outer line from the boundary $\partial\Omega$ depicts the probability that a source will be positioned at that point on the boundary – i.e. in this case it is more likely that a source is positioned at the top right of the domain than the bottom left of the domain



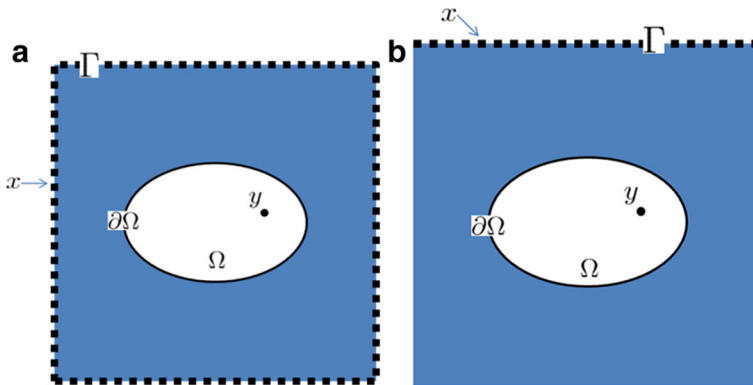


Fig. 2 Two different inspection scenarios where the dotted line represents the distribution of ultrasonic sources: (a) is referred to as a full aperture inspection and (b) is referred to as a limited aperture or single sided inspection

effects of the component shape on the ultrasonic coverage. We assume here that $\xi(x) = 1 \forall x \in \Gamma$ where Γ is the boundary of the immersion inspection domain. The outcomes of this upper level optimisation will be used to reduce the dimension of the search space and provide constraints for the lower level optimisation of the source placement (which is of course dependent on the boundary of the component).

Problem 2: Calculating optimal source placement

The component geometry $\partial\Omega$ will now be constrained by the findings of the upper level optimisation as described in Problem 1. For a given component Ω for which the material properties θ and boundary $\partial\Omega$ are known, we wish to find the optimal source placement $\xi^*(x)$

$$\xi^*(x) = \arg \max_{\xi \in \Phi(\partial\Omega)} \Psi(\xi(x); \partial\Omega), \quad (5)$$

where $\Phi(\partial\Omega)$ is the set of admissible source distributions for the given component boundary $\partial\Omega$ (thus taking into account the restrictions to the component's surface access). Using a Markov chain Monte Carlo (MCMC) method coupled with Metropolis-Hastings criterion [1], we can iterate over the model space, changing the distribution of sources $\xi(x)$ over the component's surface to maximise $\Psi(\xi(x); \partial\Omega)$. Thus we obtain a component geometry which lies within the initial design constraints and, when inspected by ultrasonic transducers placed according to $\xi^*(x)$, maximises our ability to successfully test the component non-destructively.

Simulation of the ultrasonic inspection of a given component design

Having set up this design optimisation framework for ultrasonic array NDT, we now demonstrate the effects that the source placement $\xi(x)$ and component boundary $\partial\Omega$ have on the coverage Ψ . The software package PZFlex [14] was identified as the ideal environment to examine the effects of inspection aperture and component design on the coverage of the induced ultrasonic field. Using this finite element software, we were able to simulate the ultrasonic inspection of irregularly shaped components. We initially work within a two dimensional framework. This is a fair representation of the physical scenario as ultrasonic transducers are usually placed in a single plane so that we effectively inspect a slice of the

component. However, it can be noted that PZFlex has the capability to read in computer aided design (CAD) files of 3D components [7] and so the framework developed can easily be extended to more complex inspection scenarios in the future if necessary.

In this paper, we study two different inspection scenarios. The first is a four sided inspection, where an array of sources are placed on each side of the two-dimensional square domain, enclosing the component under inspection and providing a full aperture interrogation (see Fig. 2a). The second scenario models a linear array of sources placed on a single side of the inspection domain (Fig. 2b). This single-sided inspection better represents the scenarios faced by NDT operators in industry where only a sub-region of the surface can be accessed. In both cases, the elements were fired simultaneously to induce plane waves and inject the maximum amount of energy into the system. Note that here the sources are not placed on the component boundary but are instead placed in the water surrounding the component. This is known as immersion testing and allows for testing of irregularly shaped components by standard phased array equipment.

Results

Effects of component design on ultrasonic coverage

To begin, we examine the simplest case and compare the ultrasonic coverage of a steel disc placed in water against that of a rectangular steel block placed in water (the geometries are shown in Fig. 3a and d). Initially, a one sided inspection was simulated where a plane wave was induced at the top of the domain. The wave travels through the water host until it reaches the component where some energy penetrates its surface and, due to the mismatch in impedance between the water and steel, a high proportion of the energy is reflected or redirected around the component. The results are shown in Fig. 3b and e for the rectangular block and disc respectively, and both are plotted over a dynamic range of 30 dB. The maps are quantified by the mean, variance, minimum amplitude and percentage of pixels which lie above the -20 dB threshold (see Table 1) and it can be concluded that the coverage is better in the rectangular sample. The results arising from a full aperture inspection are shown in images (c) and (f) and again, from the values in Table 1, the rectangular component exhibits a higher pressure field throughout. Note in this case however, that if we take the variance of the pressure field as a measure of the uniformity of the coverage, we observe that the disc exhibits a more even coverage than the rectangular block. However, the mean value tells us that the coverage is of lower quality in the disc case. This can be attributed to the fact that its rounded boundaries guide the pressure wave around the object, thus reducing penetration and lessening the component's coverage.

The next step in understanding important aspects of component and experimental design was to study more complex component geometries. Three examples are shown in Fig. 4a, b and c featuring irregularly shaped components. The component shown in Fig. 4a was first inspected by a single plane wave induced at the top of the domain. As most of the upper surface lies perpendicular to the wave front direction, a large proportion of the energy penetrates the surface of the component. The energy appears to concentrate in the central, narrow area of the component and high amplitudes can be observed at its inner corners. From initial observations, these inverted corners seem to trap the energy within the component by diffracting outgoing energy and redirecting it internally. The same phenomenon is observed in

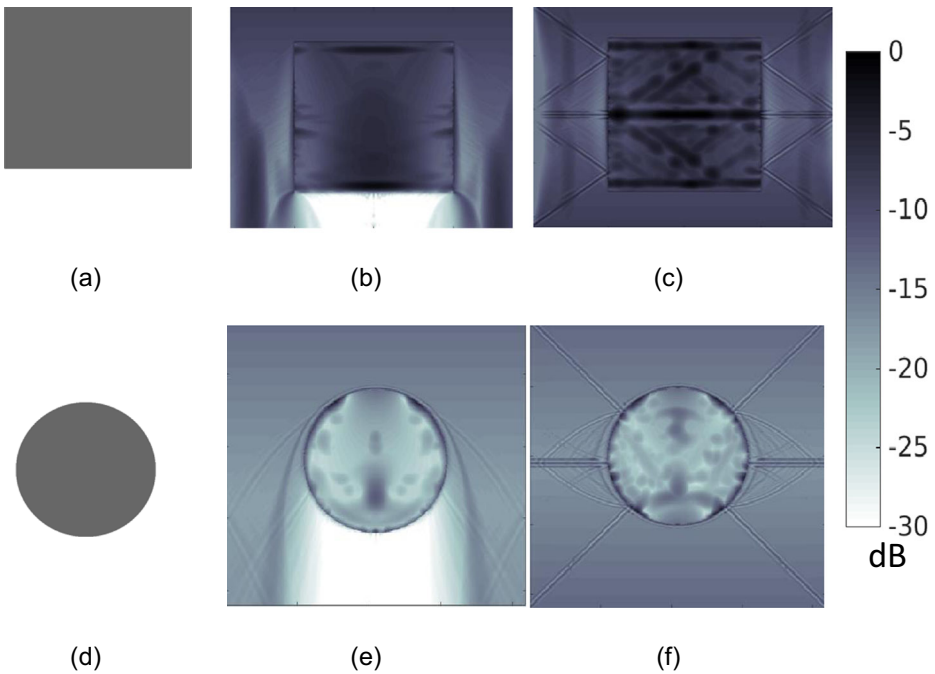


Fig. 3 The ultrasonic coverage of simple components was examined. Image (a) shows a rectangular steel block and images (b) and (c) show the maximum pressure measured at each point in the domain for the limited and full apertures respectively. Image (d) shows a steel disc and images (e) and (f) show the maximum pressure measured at each point in the domain for the limited and full apertures respectively

the full aperture case (Fig. 4g). When the corners are rounded, as in geometry 4 (b), this effect is lessened. Instead, the amplitudes are highest at the rounded surface of the component as observed previously in the disc case, and the coverage within the component deteriorates (Fig. 4e and h). Quantitative measures of the coverage are recorded in Table 2 and the values for the limited aperture and full aperture cases can be compared. Note that there is an improvement in coverage in each case when the full aperture is employed however this must be tempered by the fact that four times as much energy is entering the system.

The ultrasonic coverage was then altered by placing the sources at the left hand side of the domain. Much of the energy is trapped in the left vertical bar of the component in Fig. 4j as the wave is reflected off the inner steel-water interface. The same result is observed in the case shown in Fig. 4k, but to a lesser extent due to the curved surface (less energy is transmitted into the component to start with). In both cases, the vertical bar on the right hand side receives very little coverage and would be considered a ‘dead zone’.

Table 1 Quantitative measures of the coverage maps plotted in Fig. 3

Geometry	Inspection Aperture	Mean (dB)	Var (dB)	Min (dB)	> -20db (%)
(a) Block	Limited	-7.6	8	-17.8	100
	Full	-7	11.5	-13	100
(d) Disc	Limited	-19	9	-23.5	48
	Full	-17	9.3	-24	64

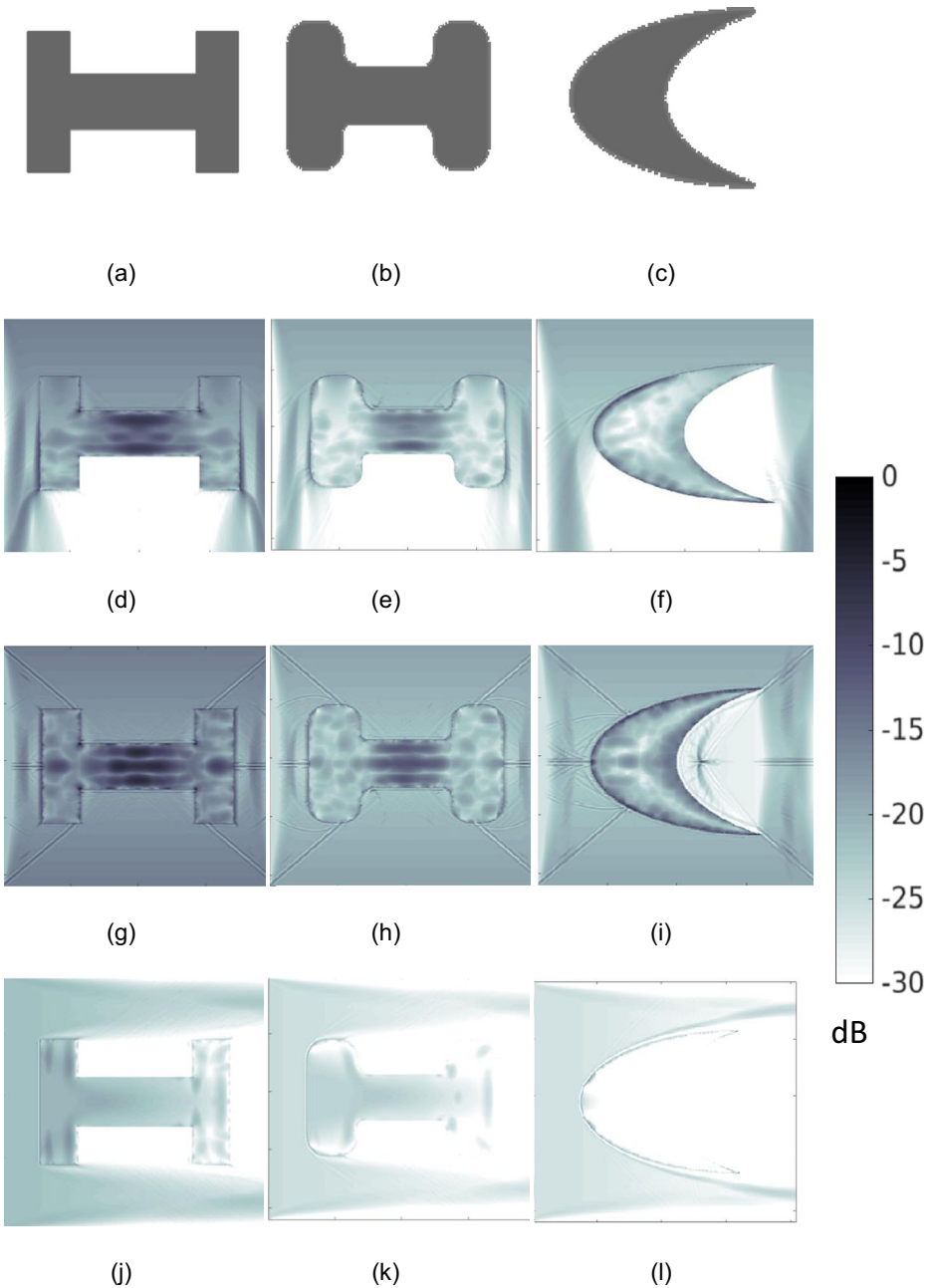


Fig. 4 Images (a–c) show the irregularly shaped components input into the finite element (PZFlex) inspection simulation. Images (d–f) plot the maximum pressure at each point in the domain for a single-sided inspection where the incident plane wave is released at the top of the domain, (g–i) for the full aperture inspection and (j–l) for the single sided inspection where the incident wave travels from left to right

Table 2 Comparing the coverage afforded by three different inspections for geometries (a), (b) and (c) in Fig. 4

	Sources at top of the domain			Full Aperture			Sources at left of domain		
	(a)	(b)	(c)	(a)	(b)	(c)	(a)	(b)	(c)
Mean (dB)	-17.3	-23	-23.7	-14.7	-20	-19.4	-23.5	-27.9	-33.8
Var (dB)	18	18.7	36.3	10.4	10.16	15.5	21.6	25.2	19.5
Min (dB)	-46	-60	-54.4	-26.2	-57	-41.1	-40.5	-62	-58
>20 dB (%)	85	21	20.4	99.3	38.2	54	7.8	0.3	0.2

Finally, a crescent shaped component was examined (Fig. 4c). As observed in all previous examples, the curved surface leads to poor coverage of the component. Naturally, when the concave curved surface is illuminated by the plane wave (as in the full aperture case shown in Fig. 4i) a focal point of energy outside of the component is created, which is detrimental to our purpose.

Discussion

It has already been shown that enhanced inspection protocols serve to reduce process waste and improve overall efficiency in the remanufacturing of complex components [20]. Currently, inspection protocols are limited in most cases to visual and scent inspections. Where more advanced inspection techniques such as fibre optic endoscopy are applied, they are still limited to superficial, surface examinations. We propose that ultrasonic inspection is most suited to assessing the structural integrity of a component's interior due to its ability to reliably detect sub surface damage, inexpensiveness, automation potential and portability. The ability to reliably detect interior damage and weaknesses will ensure that remanufacturing practices can be extended and applied to expensive components used in heavy industry which are subjected to extreme stresses on a daily basis. In fact, it has previously been reported that the only way to increase the amount of remanufacturing within the aerospace industry would be to invest in the development of more effective NDT strategies to ensure more reliable structural assessments [3].

The major challenge in integrating ultrasonic NDT within the remanufacturing process is that its deployment can be inhibited when components exhibit complex geometries or are constructed from heterogeneous media. This is particularly relevant in remanufacturing as components often feature complex geometrical features to facilitate easy disassembly. We have shown using simple examples that a component's convexity, surface smoothness and inspection aperture have a significant effect on the ultrasonic coverage and the existence of dead zones. By presenting a framework which allows original equipment manufacturers (OEMs) to account for the component's testability at the design stage, we hope that ultrasonic testing can become better integrated in the remanufacturing process at the *Receive Core* stage. It is important to note however, that ultrasonic NDT has been presented here as a secondary design constraint and so this approach will be limited by the

flexibility in the original design of the component; can the design be altered to consider the component's testability without modifying its functionality or incurring unwarranted costs? However, there are scenarios in which it would be a primary objective, trading off directly with cost and waste reduction; if the integrity of a component is critical to the safety of a product, and without NDT the safety cannot be guaranteed and hence the component cannot be remanufactured, the ability to apply NDT techniques may have a first-order effect on the component's lifetime value. Additionally, ultrasonic NDT is ineffective in detecting damage in the near field of the array and so the integration of this inspection methodology is complementary to the existing visual inspection protocols which provide an efficient and economical way of detecting surface breaking damage. Future work will focus on developing a software package based on the presented framework which quantifies a component's testability and produces designs with enhanced testability. Studies which weigh the cost benefit of the enhanced process efficiency against the additional cost incurred by implementing of ultrasonic inspection will also follow. Of course, for simply designed components, enhanced inspection will not always be economically viable and so an outstanding challenge will be in determining when this process is worthwhile.

Conclusions

The primary aim of this paper was to present a mathematical framework for including ease of NDT as a design consideration, and to demonstrate that by altering a component's shape and data acquisition geometry, the coverage of the pressure field can be adjusted. It is hoped that by considering NDT suitability in the design process, not only will the success of in service inspections be enhanced, but the range of products suitable for remanufacturing will be extended.

A multi-level optimisation scheme which maximises the coverage of the ultrasonic field by perturbing the component's shape and subsequently assessing the optimal placement of sources on the component's boundary is proposed. To better understand how these factors affect the coverage of the ultrasonic field, simulations of limited and full aperture inspection scenarios were run in the software package PZFlex. The coverage was quantified using the mean value of the coverage map, the variance, the minimum amplitude of the field and the percentage of points in the domain which lie above a threshold (chosen here as -20 dB). Five different component geometries were examined in this way and it was shown that the presence of curved boundaries prohibited the penetration of the wave energy at the surface of the component (the external pressure field flowed around the boundary), whilst surfaces parallel to the incident wave field resulted in higher amplitude coverage throughout the component. Additionally, coverage was improved when a full aperture was employed (as expected) but also varied dramatically depending on which surface lay parallel to the incident plane wave. Having proposed this framework and defined some measures for quantifying the coverage, the next step will be to implement the optimisation strategy on simple, yet industrially relevant, component geometries. The method will then be extended to include a third nested optimisation in which the distribution of the material properties θ will be considered.

Acknowledgements This work was funded by the Engineering and Physical Sciences Research Council (grant number EP/P005268/1). The authors would like to thank the team at PZFlex (Glasgow office) for their continued support.

Authors' contributions Each author contributed to the development of the novel concept central to this paper. The simulations were run by KMMT.

Data statement All results presented in this publication can be reproduced using the model made available at the University of Strathclyde KnowledgeBase at <https://doi.org/10.15129/ed8564a2-ad9f-4ba3-9769-c6a4980af17c>

Open Access This article is distributed under the terms of the Creative Commons Attribution 4.0 International License (<http://creativecommons.org/licenses/by/4.0/>), which permits unrestricted use, distribution, and reproduction in any medium, provided you give appropriate credit to the original author(s) and the source, provide a link to the Creative Commons license, and indicate if changes were made.

References

1. Aster RC, Borchers B, Thurber CH (2005) *Parameter Estimation and Inverse Problems*, Elsevier
2. Brown RH, Pierce SG, Collison I et al (2015) Automated full matrix capture for industrial processes. 41st Annual review of progress in quantitative nondestructive evaluation: volume 34.1650:1967–1976
3. Centre for remanufacturing and reuse: remanufacturing in the UK: a snapshot of the UK remanufacturing industry (2010) <http://www.remanufacturing.org.uk/pdf/story/lp342.pdf> [Accessed 08/06/18]
4. Chang Y, Bae JH, Yi HC (2013) Ultrasonic cleaning of used plastic parts for remanufacturing of multifunctional digital copier. *Int J Precis Eng Manuf* 14(6):951–956
5. Chepuri SP, Leus G (2015) Sparsity-promoting sensor selection for non-linear measurement models. *IEEE Trans Signal Process* 63(3):684–698
6. Coles D, Prange M, Djikpesse H (2015) Optimal survey design for big data. *Geophysics* 80(3):11–22
7. Dobson J, Tweedie A, Harvey G et al (2016) Finite element analysis simulations for ultrasonic array NDE inspections. 42nd Annual review of progress in quantitative nondestructive evaluation: incorporating the 6th European-American workshop on reliability of NDE, vol 1706. Melville
8. Fan C, Caleap M, Pan M, Drinkwater BW (2014) A comparison between ultrasonic array beamforming and super resolution imaging algorithms for non-destructive evaluation. *Ultrasonics* 54(7):1842–1850
9. Farkas J, Jármai K (1997) *Analysis and optimum design of metal structures*. CRC Press
10. Farkas J, Jármai K (2008) *Design and optimization of metal structures*. Elsevier
11. Hammond R, Amezquita T, Bras B (1998) Issues in the automotive parts remanufacturing industry: a discussion of results from surveys performed among remanufacturers. *Eng Des Autom* 4:27–46
12. Hatcher GD, Ijomah WL, Windmill JFC (2011) Design for remanufacture: a literature review and future research needs. *J Clean Prod* 19(17):2004–2014
13. Ijomah WL, McMahon CA, Hammond GP, Newman ST (2007) Development of design for remanufacturing guidelines to support sustainable manufacturing. *Robot Comput Integr Manuf* 23:712–719
14. Koul AK, Castillo R (1988) Assessment of service induced microstructural damage and its rejuvenation in turbine blades. *Metall Trans A* 19(8):2049–2066
15. Liu W, Zhang B, Li MZ, Li Y, Zhang HC (2013) Study on remanufacturing cleaning technology in mechanical equipment remanufacturing process. In *Re-engineering manufacturing for sustainability*, Springer, Singapore, p 643–648.
16. Lund RT (1984) Remanufacturing: the experience of the U.S.A. and implications for the developing countries. World bank technical paper No. 3
17. Mosch M, Oster R, Grosse CU (2016) Non-destructive testing of CFRP in the design process—a generic approach to describe and optimize non-destructive testing. In 19th WCNDT, Munich, Germany
18. PZFlex (2017) Thornton Tomasetti Defence Ltd 6th Floor South, 39 St Vincent Place, Glasgow, Scotland, G1 2ER, United Kingdom
19. Raj B, Jayakumar T, Thavasimuthu M (2002) *Practical non-destructive testing*. Woodhead Publishing
20. Ridley S.J. (2012) Improving the efficiency of the remanufacture of complex mechanical assemblies with robust inspection of core units. In: Matsumoto M, Umeda Y, Masui K, Fukushige S. (eds) *Design for innovative value towards a sustainable society*. Springer, Dordrecht, ISBN 978–94–007–3010–6

21. Ridley SJ (2013) Increasing the efficiency of engine remanufacture by Optimising pre-processing inspection – a comprehensive study of 2196 engines at Caterpillar remanufacturing in the UK. PhD Dissertation: The University of Strathclyde
22. Scherrer LW (2016) Fundamentals of ultrasonic nondestructive evaluation. Springer
23. Shingo S (1986) Zero quality control: source inspection and the poka-yoke system. CRC Press
24. Tant KMM, Galetti E, Mulholland AJ, Curtis A, Gachagan A (2018) A Transdimensional Bayesian Approach to Ultrasonic Travel-time Tomography for Non-Destructive Testing. *Inverse Problems* 34(9): 095002

Affiliations

Katherine M. M. Tant¹ • **Anthony J. Mulholland**¹ • **Andrew Curtis**² • **Winifred L. Ijomah**³

Anthony J. Mulholland
anthony.mulholland@strath.ac.uk

Andrew Curtis
andrew.curtis@ed.ac.uk

Winifred L. Ijomah
w.l.ijomah@strath.ac.uk

¹ Department of Mathematics and Statistics, University of Strathclyde, Livingstone Tower, Richmond Street, Glasgow, UK

² School of Geosciences, Grant Institute, University of Edinburgh, Kings Buildings, Edinburgh, UK

³ Department of Design, Manufacture and Engineering Management, University of Strathclyde, James Weir Building, Montrose Street, Glasgow, UK